Refined Energy Correction for Calibration of Submerged Radial Gates

Tony L. Wahl, P.E., M.ASCE[1]

Abstract: The energy-momentum (*E-M*) method for calibrating submerged radial gates was refined using a large laboratory data set collected at the Bureau of Reclamation hydraulics laboratory in the 1970s. The original *E-M* method was accurate in free flow, and when the gate significantly controls submerged flow, but for large gate openings with low head loss through the gate, discharge prediction errors were sometimes large (approaching 70%). Several empirical factors were investigated with the laboratory data, including the combined upstream energy loss and velocity distribution factor and the submerged flow energy correction. The utility of the existing upstream energy loss and velocity distribution factor relation was extended to larger Reynolds numbers. The relation between the relative energy correction and the relative submergence of the vena contracta was shown to be sensitive to the relative jet thickness. A refined energy correction model was developed, which significantly improved the accuracy of submerged flow discharge predictions. Although the focus of this work was radial gates, the energy correction concept and these refinements potentially have application to all submerged sluice gates.

DOI: 10.1061/(ASCE)0733-9429(2005)131:6(457)

CE Database subject headings: Gates; Discharge coefficients; Discharge measurement; Submerged discharge; Submerged flow; Submerged jets; Hydraulic jump.

Introduction

Radial gates are common features of most irrigation projects. The ability to accurately measure discharge through these structures would allow project operators to more effectively deliver water to end users in a timely and accurate manner, and would reduce the need for the construction of separate dedicated flow measurement structures. The calibration of radial gates for flow measurement is a challenging hydraulic problem due to the number of possible gate, structure, and channel configurations, and the sensitivity of calibrations to such factors as gate seal type and downstream channel width. Calibration methods for gates operating in a free-flow condition are available in standard references and have reasonable accuracy and ease of use, but calibrations for submerged gates are often very inaccurate, with errors of up to 50% reported. Most available calibration methods rely primarily on the energy equation, although some incorporate the momentum equation to distinguish between free- and submerged-flow conditions.

A procedure that uses both the energy and momentum equations for flow calibration was recently developed (Clemmens et al. 2003). The energy-momentum (*E-M*) method uses an iterative solution of the energy and momentum equations and offers several potential advantages over previous methods:

- Ability to account for differing upstream and downstream channel widths and differing channel invert elevations relative to the gate sill,
- Potentially better accuracy when structures include multiple gates that are not operated uniformly, and
- Accurate determination of free- and submerged-flow conditions and accurate calibration continuously through free-flow, transition, and submerged-flow conditions.

The *E-M* method is theoretically based, but also makes use of empirical relations for gate contraction coefficients, energy loss, and velocity distribution factors in free flow, adjustments to the energy equation in submerged flow, and hydrostatic forces on downstream channel boundaries. The initial empirical relations were developed from a series of experiments performed by the Agricultural Research Service (ARS) at the U.S. Water Conservation Laboratory, Phoenix, (Tel 2000). These experiments used a single radial gate structure with a sharp-edged gate leaf. In free-flow conditions the experiments covered a broad range of gate openings, but in submerged-flow conditions the tests were performed at only one gate opening with four different flow rates and a range of tailwater conditions. The submerged flow tests covered an intermediate range of relative gate openings (the ratio of gate opening to upstream head), but did not include very small or very large relative gate openings. Despite the limited data, performance of the method has thus far been encouraging, but there is a great need for testing against other data sets, especially over a wider range of submerged-flow conditions. Clemmens et al. (2003) speculated that the relative gate opening might be a crucial parameter affecting submerged-flow calibration.

A series of tests performed at the Bureau of Reclamation hydraulic laboratory in Denver, Colorado (Buyalski 1983) offers an opportunity to test the *E-M* method over a wide range of conditions and possibly refine some of its empirical components. Buyalski's data were originally used to develop an energy-based calibration method, which was implemented in the *RADGAT*

[1]Hydraulic Engineer, U.S. Dept. of the Interior, Bureau of Reclamation, Water Resources Research Laboratory, Denver, CO. E-mail: twahl@do.usbr.gov

Note. Discussion open until November 1, 2005. Separate discussions must be submitted for individual papers. To extend the closing date by one month, a written request must be filed with the ASCE Managing Editor. The manuscript for this paper was submitted for review and possible publication on September 23, 2003; approved on August 24, 2004. This paper is part of the ***Journal of Hydraulic Engineering***, Vol. 131, No. 6, June 1, 2005. ©ASCE, ISSN 0733-9429/2005/6-457–466/$25.00.

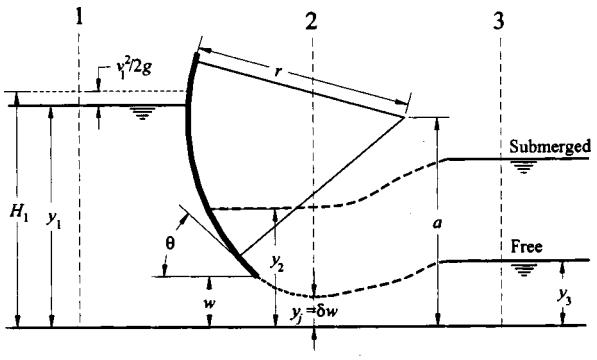

Fig. 1. Definition sketch for flow through a radial gate

computer program. Buyalski tested nine gate configurations composed from three seal configurations (sharp-edged, hard rubber bar, and music note or "J" seal), and three different ratios of gate radius to trunnion pin height. Seven different gate openings were tested for each configuration, with gate opening to trunnion height ratios varying from 0.1 to 1.2. Nearly 2,650 test runs were made, in both free and submerged conditions. The availability of both free- and submerged-flow data for the same gates makes it possible to analyze the data in several ways to determine contraction coefficients and other empirical factors in the *E-M* method. Buyalski also collected more than 450 data points from 13 prototype gates for use in a field verification program.

Unfortunately, all but one prototype site operated only in submerged flow, and the other operated in free flow only. Thus, it would be much more difficult to isolate the various empirical parameters in the same way as can be done with the laboratory data. Also, at most of the prototype sites, current metering methods were used for independent discharge measurement, so uncertainties in the measured data are much greater than in the laboratory data.

This paper uses the Buyalski laboratory data set to test the *E-M* method as proposed by Clemmens et al. (2003), and then presents modifications to incorporate the relative gate opening and its influence on the submerged-flow energy correction term.

Methods

The *E-M* calibration method is described in detail by Clemmens et al. (2003). To provide a basis for the analysis and discussion that follow, the method is briefly reviewed here as originally proposed. Later, modifications to improve the model are presented in the section entitled, "Analysis and Results."

The *E-M* equations are applied to the flow situation shown in Fig. 1. The energy equation is applied to the flow from Section 1 to Section 2, and the momentum equation is applied to the flow from Section 2 to Section 3. For free flow, only the energy equation is needed to determine the flow calibration of the gate. Key parameters are those shown in Fig. 1, and the contraction coefficient, δ, for the flow beneath the gate, $\delta = y_j/w$, where y_j is the jet thickness at the vena contracta; and w is the vertical gate opening. In the experiments conducted by ARS, Tel (2000) found that the contraction coefficient from a sharp-edged gate was a function of the gate leaf angle, θ, at the edge of the opening

$$\delta = 1.001 - 0.2349\theta - 0.1843\theta^2 + 0.1133\theta^3 \quad (1)$$

with θ given in radians. This equation closely matches the experimental results of Toch (1955) and others, summarized in Clemmens et al. (2003).

Free Flow

Clemmens et al. (2003) wrote the energy equation from Section 1 to 2 using the free-flow jet velocity at the vena contracta

$$H_1 = H_j + \Delta H = y_j + \alpha_j \frac{v_j^2}{2g} + \xi \frac{v_j^2}{2g} \quad (2)$$

where H_1=energy head at Section 1; H_j=energy head at the vena contracta (Section 2); ΔH=head loss between Sections 1 and 2; y_j=flow depth at the vena contracta, v_j=average jet velocity; α_j=velocity distribution coefficient for the jet; g=acceleration of gravity; and ξ=energy loss coefficient. The velocity distribution coefficient α_j was assumed to be 1.0, with any deviation from unity accounted for in ξ, making $1+\xi$ a combined energy loss and velocity distribution factor. Noting that the discharge is $Q = \delta w b_c v_j$, where $y_j = \delta w$ and b_c is the gate width, one may substitute for v_j and y_j in Eq. (2) and solve for discharge to obtain

$$Q = \delta w b_c \sqrt{\frac{2g(H_1 - \delta w)}{1+\xi}} \quad (3)$$

The energy loss and velocity distribution factor $1+\xi$ was related to the Reynolds number of the flow at the upstream face of the gate. In the laboratory tests (Tel 2000), values of $1+\xi$ varied from about 1.04 to 1.12 in tests covering a Reynolds number range of about 0.5×10^5 to 2.7×10^5. Clemmens et al. (2003) developed a relation between $1+\xi$ and the Reynolds number,

$$1 + \xi = 1 + 0.15e^{-5\times10^{-6}\mathrm{R}} \quad (4)$$

where e=base of natural logarithms. The Reynolds number is $\mathrm{R} = VR_h/\nu$, where ν is the kinematic viscosity, V is the characteristic velocity determined at the gate opening, $V = Q/(b_c w)$, and R_h is the hydraulic radius just upstream from the gate, between the gate piers, $R_h = b_1 y_1/(b+2y_1)$. The upstream channel width is b_1, and y_1 is the upstream flow depth. Using this model, the value of $1+\xi$ approaches 1.0 at large Reynolds numbers.

Submerged Flow

For submerged flow, the energy equation is applied from Section 1 to 2 and the momentum equation is applied from Section 2 to 3. Application of the momentum equation requires estimates of flow forces on the boundaries of the downstream channel, which are given by empirical relations developed from the ARS experiments.

Clemmens et al. (2003) described how the transition into submerged flow causes a thickening of the jet issuing from beneath the gate, accompanied by a velocity reduction. These changes take place as a result of the incomplete hydraulic jump against the downstream side of the gate and the associated adverse pressure gradient. Rather than model the actual changes in jet thickness and velocity, they proposed an alternative approach, modifying the energy equation to include an energy correction term E_{corr} that accounts for the reduced velocity head of the jet. The energy equation is then written as

$$H_1 = y_2 + \alpha_j \frac{v_j^2}{2g} + \xi \frac{v_j^2}{2g} - E_{\text{corr}} \quad (5)$$

where y_2=flow depth at the now submerged vena contracta location. The value of v_j is held constant at its free-flow value. E_{corr} is zero under free-flow and fully submerged conditions, but varies with the relative submergence of the jet in the transition zone, as shown by Clemmens et al. (2003). Eq. (5) can be solved for discharge, as described previously for free flow, again assuming that $\alpha_j = 1$

$$Q = \delta w b_c \sqrt{\frac{2g(H_1 - y_2 + E_{\text{corr}})}{1 + \xi}} \quad (6)$$

Clemmens et al. (2003) performed submerged-flow tests at a single gate opening and a range of flow rates and tailwater levels to determine values of the energy correction. They found it helpful to examine the energy correction relative to the increase in flow depth at the vena contracta, $y_2 - y_j$, and the jet thickness y_j. They related the relative energy correction, $E_{\text{corr}}/(y_2 - y_j)$, to the relative depth increase $(y_2 - y_j)/y_j$ and developed the predictive equation

$$\frac{E_{\text{corr}}}{(y_2 - y_j)} = 0.52 - 0.34 \arctan\left[7.89\left(\frac{y_2 - y_j}{y_j} - 0.83\right)\right] \quad (7)$$

[It should be noted that a bracket was misplaced in this equation in the original publication of Clemmens et al. (2003).] Eq. (7) does not include any influence of the relative gate opening, w/H_1, but Clemmens et al. (2003) speculated that with additional data a family of curves might be defined relating the relative energy correction and the relative depth increase for different values of w/H_1.

In the ARS tests, y_2 was determined from pressure measurements made in the jet with a Prandtl tube. However, y_2 is very difficult to measure in the field due to large velocities and turbulence. To address this, the downstream depth, y_3, is measured, and the momentum equation is used to relate y_2 and y_3. The momentum equation can be written as

$$Q v_e + b_c g \frac{y_2^2}{2} + \frac{F_w}{\rho} = Q v_3 + \frac{F_3}{\rho} \quad (8)$$

where v_e=effective velocity in the jet; ρ=fluid density; F_3 =hydrostatic pressure force exerted by the downstream water depth; and F_w=streamwise component of the force of water on all surfaces between Sections 2 and 3, including hydrostatic forces on all walls. Clemmens et al. (2003) discuss the effective velocity and other application details. Briefly, the effective velocity accounts for the increased thickness and reduced velocity of the submerged jet discussed earlier, which is accounted for by the E_{corr} term in the energy equation and must also be accounted for in the momentum equation. The hydrostatic force F_w is computed from an effective water depth, y_w, computed as a weighted average of y_2 and y_3

$$y_w = p y_3 + (1 - p) y_2 \quad (9)$$

The ARS tests were used to determine the empirical weighting factors for y_2 and y_3, and a value of $p = 0.643$ was obtained for their specific gate and downstream channel configuration.

Solution Procedure

The equations presented above must be solved iteratively to determine the flow rate through a gate. In free flow, iteration is required because of the Reynolds number dependence of $1+\xi$. After a free-flow discharge is computed, the momentum equation is used to determine whether the gate is submerged. If so, the momentum equation and submerged-flow energy equation are solved iteratively until y_2 and Q converge. The energy correction term and effective velocity are incorporated into the solution process.

For the analysis discussed in this paper, a Visual Basic computer program was written to process the data from the Buyalski laboratory tests. The program is able to perform the *E-M* method calculations to compute flow rate, and is also able to solve in reverse for several different parameters. First, for free-flow situations, the program can solve for the gate contraction coefficient that would produce perfect agreement between the observed discharge and the computed discharge from Eq. (3), assuming that Eq. (4) for $1+\xi$ is valid. Second, also in free flow, assuming that the gate contraction coefficient is known, the program can solve for the value of $1+\xi$ that would produce the perfect agreement of observed and computed discharge. Finally, in submerged-flow cases, the program can solve for the value of E_{corr} (and the accompanying values of y_2, y_j, and v_e) that produces perfect agreement of discharge, assuming that relations for the contraction coefficient and $1+\xi$ are given. In submerged flow, the program assumes that the empirical weighting factors for the y_w depth calculation are those obtained by Clemmens et al. (2003). These weighting factors appeared to be correct in that they properly identified free versus submerged flow in almost all cases. This is discussed in more detail later in the paper.

Table 1. Radial Gate Configurations Tested by Buyalski (1983)

Gate designation	Trunnion pin height (mm)	Seal design
1[a]	461	Hard rubber bar
2	511	Hard rubber bar
3	409	Hard rubber bar
4	409	Music note
5	461	Music note
6	511	Music note
7	409	Sharp edge
8	461	Sharp edge
9	511	Sharp edge

[a]Gate designations are correct. The tests with the hard rubber bar seal were performed in a different order than the later tests.

Buyalski Data

Buyalski (1983) tested one radial gate configured in nine different ways through a combination of three trunnion height settings and three different types of gate seals. He identified these tests as shown in Table 1. Sketches of the laboratory model gate seals are shown in Fig. 2. Detailed drawings of Buyalski's test flume and the prototype and laboratory model gate seals can be found in Figs. 7, 9, and 10 of his report, which is available online [see Buyalski (1983)].

For all tests, the gate arm radius was 702 mm (2.302 ft) and the gate width was 711 mm (2.333 ft). The upstream and downstream channel widths (at the locations where y_1 and y_3 were measured) were 762 mm (2.50 ft). The 51 mm (2 in.) difference between the gate width and the channel width was due to half-pier installed on one side of the laboratory flume. The floor of the test flume was level throughout its length. The channel approaching

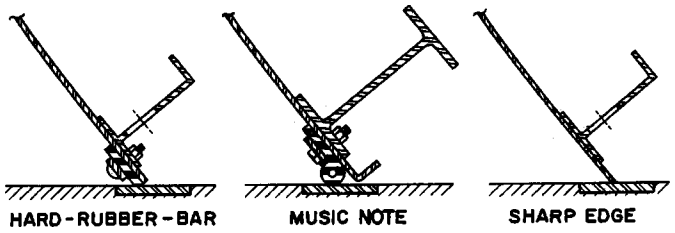

Fig. 2. Radial gate seals [after Buyalski 1983, Fig. 9(b)]

the gate was 3.12 m long (10.25 ft) and the tailwater channel was 8.46 m long (27.75 ft). An adjustable picket fence tailgate was used to regulate downstream water levels. Data were collected at six different gate openings (seven gate openings for Gates 1, 2, and 3), corresponding to nominal gate opening to trunnion height ratios of 0.1, 0.2, 0.4, 0.6, 0.8, 1.0, and 1.2 (only for Tests 1–3). The greatest volume of data (about 1,200 of the 2,650 runs) was collected from Gate 1.

Data collection consisted of discharge, water level, and pressure measurements. For each test, the flow condition was described as FREE, SUBMERGED, or JUMP (assumed to mean the flow was in the transition zone). The upstream water level, y_1, was measured 1.22 m (4 ft) upstream from the gate seal position, at a section where the channel width was 762 mm (2.50 ft). The downstream water level, y_3, was measured 3.05 m (10 ft) downstream from the gate seal position in free flow and 5.49 m (18 ft) downstream in submerged flow, again in sections where the channel width was 762 mm (2.5 ft). Pressures were measured at 25 locations along the centerline of the channel floor between 0.3 m (1 ft) upstream from the gate and 0.9 m (3 ft) downstream from the gate. Pressures also were measured at the four locations on the sidewalls of the test section just downstream from the gate leaf, and at three locations on the gate leaf itself. The floor pressure measurements would be useful for determining values of y_2 and the contraction coefficient δ, but unfortunately they could not be located. Only the upstream and downstream water level measurements were included in the final report (Buyalski 1983).

The downstream water levels, y_3, reported by Buyalski were adjusted "to an equivalent depth for a rectangular channel having a width equal to the model gate width." Buyalski reported that this adjustment was necessary to eliminate the effect of the half pier. The upstream depths were not adjusted. Because the *E-M* method applies the momentum equation between Sections 2 and 3 and thus accounts for wall forces applied by the pier, it was necessary to adjust Buyalski's reported downstream depths back to the original values that would have been measured downstream from the half pier. This allows accurate application of the momentum equation to the actual measured data. This adjustment was made using the energy equation, assuming no head loss in the expansion from the 711 mm (2.333 ft) width to the 762 mm (2.50 ft) width (believed to be the reverse of the adjustment made by Buyalski, although his report does not give details).

Evaluation of Original Energy-Momentum Model

Before making modifications to the *E-M* model, the free- and submerged-flow data from the sharp-edged gates (Gates 7, 8, and 9) were used to test the *E-M* model as originally proposed by Clemmens et al. (2003).

Discharge predictions for the free flow cases were very good. In 79% of the cases, the predicted and observed discharge were within ±2% of one another, and in 99% of the cases, the predicted and observed discharge were within ±4% of one another. The mean relative error was +0.22%, and the standard deviation of the relative errors was 1.48%. Errors were biased slightly positive (predicted flow greater than observed flow) for larger discharges.

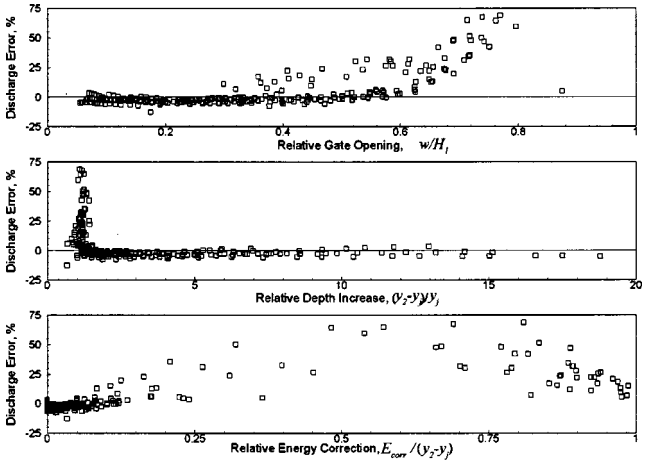

Fig. 3. Errors in prediction of submerged flow through sharp-edged radial gates

Discharge prediction for the submerged flow cases was good at small gate openings, but poor for low flows at larger gate openings where submergence is slight and the gate exerts little control on the flow. Errors ranged from −13 to +70%. Despite the fact that there were some large prediction errors, 25% of the submerged flow cases were modeled with an error in the range of ±2%, 66% had errors in the range of ±5%, and 80% had errors in the range of ±10%. The mean relative error was +4.80%, but this was strongly influenced by a few large positive errors; the median error was −1.48%. The standard deviation of the relative errors was 15.3%, again heavily influenced by a few large errors. One test failed to converge numerically (Gate model 9, Test 113, for which $w/H_1=0.88$).

Fig. 3 shows the submerged flow errors as a function of the relative gate opening, w/H_1, the relative depth increase at the jet, $(y_2-y_j)/y_j$, and the relative energy correction, $E_{\text{corr}}/(y_2-y_j)$. The largest flow measurement errors occurred for $w/H_1>0.3$, and for $(y_2-y_j)/y_j=0$ to 1.5. Thus, the flow condition producing large errors is relatively low submergence (i.e., transition zone flow) at gate openings that are a large fraction of the upstream head. This is consistent with the findings of Clemmens et al. (2003) who noted that data were lacking for large relative gate openings, and that the largest errors occur when the flow is in the transition zone, where $E_{\text{corr}}/(y_2-y_j)$ is in the range of $\sim 0.2-0.8$ and is changing rapidly as a function of the relative increase in jet thickness. There is a slight, but noticeable negative bias (predicted flows too low) for highly submerged-flow conditions, reflected in the difference between the mean and median errors discussed above.

It should be noted that low submergence in this context means only that the downstream flow depth is not dramatically greater than the theoretical free-jet thickness for a given gate opening. For a large relative gate opening, the submergence by this definition can be low at the same time that the downstream depth is almost equal to the upstream depth, a condition that would be described as large submergence by those familiar with the submergence definition used for flumes and weirs.

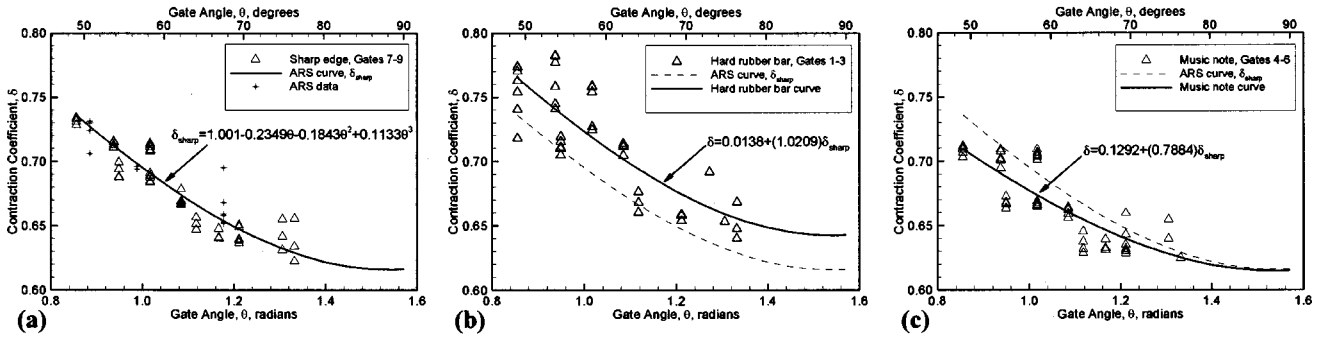

Fig. 4. Contraction coefficients of gates tested by Buyalski compared to relation for sharp-edged gates determined in Agricultural Research Service tests

Analysis and Results

The analysis objective was to use portions of the Buyalski laboratory data set to verify and/or improve the empirical relations previously developed by Clemmens et al. (2003), especially the submerged-flow energy correction term. At each step, the existing empirical relations were used within previously established ranges and attempts were made to verify, extend, or improve the relations for use in other ranges (e.g., at larger Reynolds numbers). The sequence of steps taken was as follows:

1. Use free-flow data at low Reynolds numbers to compute contraction coefficients for the three gate seal types tested by Buyalski (sharp edge, hard rubber bar, and music note seal).
2. Use contraction coefficients from Step 1 and free-flow data to examine behavior of $1+\xi$ at larger Reynolds numbers.
3. Confirm value of p, the empirical weighting factor for computing hydrostatic forces on downstream channel boundaries, by determining whether the *E-M* method correctly predicts whether flows in Buyalski's tests were free or submerged.
4. Use submerged-flow data for gates with sharp edges and hard rubber bar seals to compute values of E_{corr}, making use of the results from Steps 1 through 3. Examine the relationship between E_{corr} and the relative gate opening, and refine the model for computing E_{corr}.
5. Test the refinements by attempting to predict discharge for the Buyalski tests of gates with music note seals.

Contraction Coefficients

The analysis began with the assumption that the upstream head loss and velocity distribution factor, $1+\xi$, could be computed from Clemmens' relation [Eq. (4)] for tests in which the gate entrance Reynolds number was less than 2.7×10^5 [the upper limit of Tel's data, used to develop Eq. (4)]. This made it possible to use the Buyalski free-flow data to solve for the contraction coefficients in the free-flow tests conducted at $R<270{,}000$. Contraction coefficients for the hard rubber bar and music note seals were compared to the contraction coefficients for the sharp-edged gate, as given by Eq. (1), and regression relations for the ratios of the contraction coefficients were developed as a function of the gate angle, θ. This yielded the following relationships (Fig. 4):

$$\delta_{sharp} = 1.001 - 0.2349\theta - 0.1843\theta^2 + 0.1133\theta^3 \quad (10)$$

$$\delta_{hard\ rubber\ bar} = 0.0138 + (1.0209)\delta_{sharp} \quad (11)$$

$$\delta_{music\ note} = 0.1292 + (0.7884)\delta_{sharp} \quad (12)$$

These relationships are based on free-flow tests conducted at angles of $\theta<1.35$ radians (77°). Buyalski tested larger gate openings (up to 98°) in submerged flow, but could not produce free flow at gate openings greater than 77°. The ARS relation for δ_{sharp} predicts increasing contraction coefficients when θ is greater than 90° (1.571 radians). This is contrary to the physics of the flow situation (more flow contraction would be expected when the flow must turn a corner greater than 90°). For this reason, and because submerged operation at such large gate openings is not a common field practice, Buyalski's data for $\theta>90°$ were discarded in the remainder of this analysis (35 tests), but his submerged-flow data up to $\theta=90°$ were used, making use of Eqs. (10)–(12) to compute contraction coefficients. For the sharp-edged gates, the data fit the ARS relation [Eq. (1)] closely enough that it was used without modification as Eq. (10)

The general trend in Fig. 4 is $\delta_{music\ note}<\delta_{sharp}<\delta_{hard\ rubber}$. This makes sense physically, since the music note seal is relatively thick compared to the other two cases (see gate seal sketches in Fig. 2). The bulb is thickest very near the controlling edge and forces the streamlines away from the gate face just before they begin turning the corner around the seal. Thus, a larger change in flow direction must be accomplished, which yields more contraction and a smaller contraction coefficient. This effect seems to decrease as the gate angle increases, which makes sense because at larger gate angles the flow approaching the gate lip is less aligned with the face of the gate, so the additional contraction caused by the thick bulb is reduced. In contrast, the hard rubber bar seal is much thinner than the bulb of the music note seal, and the seal is held in place by a clamp bar that is set back slightly from the controlling edge of the seal. The flow can align itself with the face of this clamp bar, and then the flow can actually begin to make its turn around the clamp bar before reaching the edge of the seal itself. This, combined with the fact that the edge of the rubber bar is likely to be somewhat rounded itself, causes less contraction (a larger coefficient) than for the sharp-edged gate.

Energy Loss and Velocity Distribution Factor

The second step of the analysis was to use the newly developed contraction coefficient relations and the free-flow data for $R>270{,}000$ to examine the relation for the upstream energy loss and velocity distribution factor, $1+\xi$ [Eq. (4)], at large Reynolds numbers. Data from all three gate seal types were used. This may

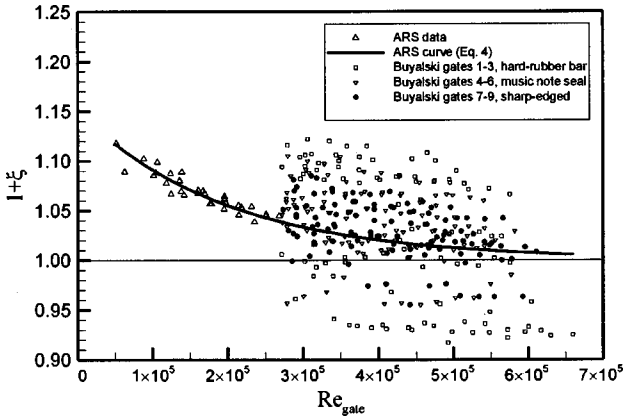

Fig. 5. Combined energy loss and velocity distribution factor

at first seem to be a circular argument, since we are using the contraction coefficients we just determined by assuming that Eq. (4) was applicable. However, it should be carefully noted that different data sets segregated by Reynolds number are being used. We only applied Eq. (4) in the previous section to a range of data for which its validity is already well established (Clemmens et al. 2003). The contraction coefficients determined from that analysis can now be used here, since they do not vary with Reynolds number.

The free-flow equations were solved in reverse to determine the values of $1+\xi$, and the results are shown in Fig. 5. The spread of the Buyalski data is much greater than that of the ARS data; in fact, values less than 1 were computed for many cases, which do not make theoretical sense. Despite the scatter in the Buyalski data, Fig. 5 appears to confirm that Eq. (4) is applicable to larger Reynolds numbers.

After careful investigation, it was found that the errors visible in Fig. 5 are related to some degree to gate setting. Buyalski's gate openings were set by lowering the gate onto a pair of machined blocks and then clamping the gate in place for a complete series of tests. Despite this care, a series of tests run on a given gate at the same gate opening often plot somewhat below or above the curve defined by Eq. (4), but with a similar shape. This suggests an error in the gate opening, or perhaps another parameter common to a series of tests at a given gate opening. The problem appears to be greater on the gates with seals, so seal compression on the positioning blocks may have been a factor, although the variability appears more random than biased. Another possibility is the variation in the accuracy of the venturi meters used to measure discharge. Venturi meters ranging from 75-mm (3-in.) to 356-mm (14-in.) diameter were used, and tests at low gate openings probably used smaller venturi meters, while those at larger gate openings would have used the larger venturi meters (specific meters were not identified for each test). Bias errors in individual venturi meter calibration could thus show up as systematic errors related to gate opening. Buyalski's venturi meters were calibrated using a volumetric tank, with an uncertainty of about ±0.5%. For comparison, discharge measurements in the ARS tests had an uncertainty of about ±0.1%, using a weigh tank. Thus, both gate setting and discharge measurement are possible sources of the additional scatter in Buyalski's data. For tests at one stated gate opening, the errors are primarily systematic, but over the course of thousands of tests the errors are random, as shown in Fig. 5, so they should not dramatically affect the conclusions drawn from these analyses.

Downstream Wall Depth Weighting Factor

The next stage of the analysis was to verify the value of the parameter p used to estimate wall forces in the momentum equation. A value of $p=0.643$ was obtained from the ARS tests (Clemmens et al. 2003), by solution of the momentum equation from measured values of y_2 and y_3. The Buyalski data set does not offer the same opportunity to solve for p, since y_2 was not measured independently. The only test that is possible is to determine whether the momentum equation correctly predicts free- and submerged-flow conditions for the Buyalski tests. If there are runs that are not correctly modeled, then one could hypothesize that the run in question was exactly at the transition from free to submerged flow and solve the momentum equation in reverse to determine the value of p that balances the momentum equation.

The Buyalski free- and submerged-flow data sets for all gate configurations and Reynolds numbers (except gate openings greater than 90°) were processed to determine whether the *E-M* method would accurately identify the flow as free or submerged. The momentum force of free flow through the gate is compared to the momentum force associated with the measured tailwater. If the tailwater force is greater, the flow is submerged; if the tailwater force is smaller, the flow is free and a hydraulic jump occurs downstream from the gate.

A total of 458 runs were examined that had been described by Buyalski as FREE, and 454 were correctly identified as free flow using the *E-M* method. The four cases that were identified as submerged flow were initially perplexing because the y_3 depth was less than the gate opening. A closer investigation showed that the momentum equation was unbalanced because the reported y_3 depth was too low, causing the Qv_3 term in the momentum equation to become extremely large. A very slight increase in y_3 caused the flow to be correctly modeled as free.

The submerged-flow data were tested in a similar manner. A total of 2,101 runs that were described by Buyalski as SUBMERGED were analyzed, and 40 of these runs were identified by the *E-M* method as free flow. For these cases, an attempt was made to compute values of p that would balance the momentum equation and cause the *E-M* method to predict submerged flow. For all 40 cases, the computed value of p was greater than 1.

In addition to free and submerged flows, Buyalski reported 63 tests having a flow condition described as JUMP. This is assumed to mean that the flow is in the transition zone, but it is not clear whether we should expect such flows to be modeled as free or submerged when examined with the momentum equation. It was hoped that these tests might provide conditions in which the momentum equation would be almost perfectly balanced and might give an opportunity to solve for p at the balanced condition. These 63 tests were analyzed, with 44 initially identified as free and 19 identified as submerged. The momentum equation was then solved to determine the balancing value of p for each case. In 39 cases, the balancing value of p was a complex number, in 21 cases, p was negative, in two cases p was greater than 1, and in one case p was equal to 0.46.

In summary, in almost every case, physically unreasonable values of p were needed to balance the momentum equation. This suggests that the tests were not actually close enough to the transition flow condition, or that other random experimental errors were unbalancing the momentum equation to a greater degree than could be accounted for by changing p within a reasonable range.

One might have expected that a lower value of p would be appropriate for Buyalski's tests, since the channel was much nar-

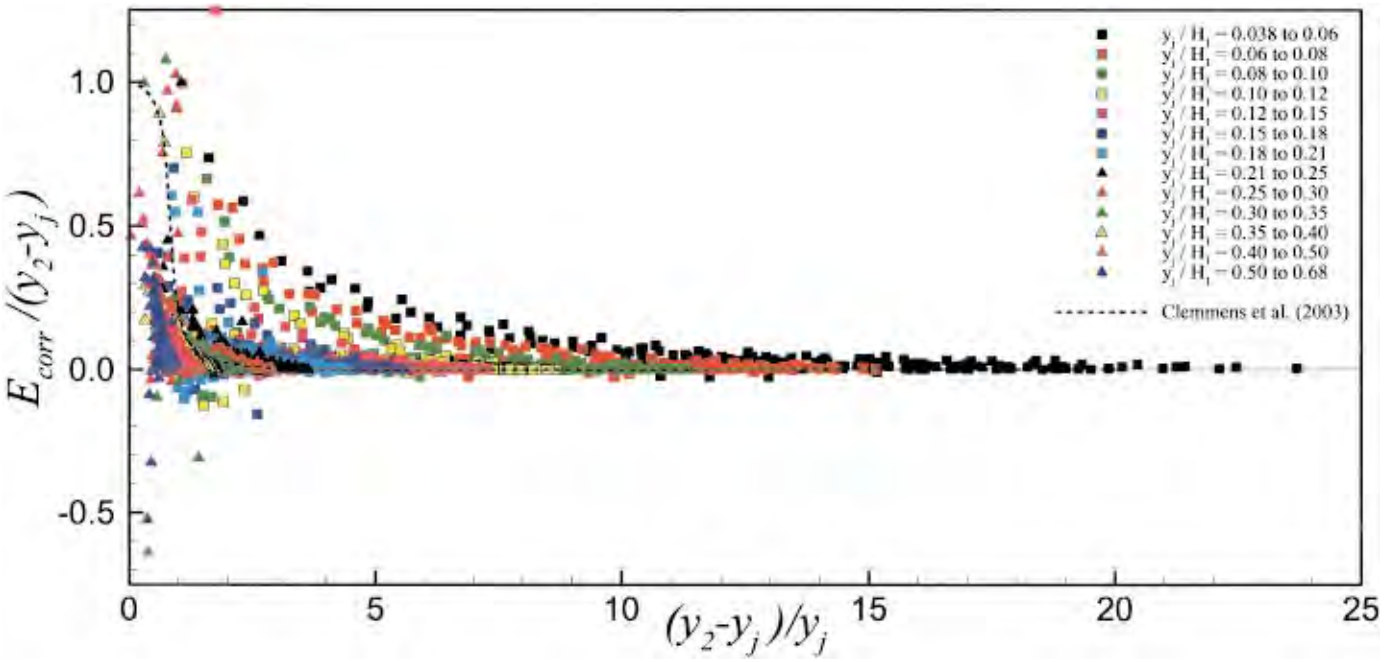

Fig. 6. (Color) Relative energy correction versus relative depth increase, subdivided by y_j/H_1 ranges

rower than that used by Tel (2000). Buyalski's downstream channel was only 7% wider than the gate, whereas Tel's was 2.7 times the width of the gate. In a narrower channel, one would expect the downstream depth, y_3, to have less influence on the forces exerted on and by the transitional sidewalls surrounding the gate, since there is less room for eddies and recirculation. This expectation was fulfilled by the one run in which $p=0.46$ balanced the momentum equation. However, one data point was felt to be insufficient evidence to warrant changing the value of p.

Energy Correction Factor in Submerged Flow

The next stage of the analysis was to determine values of E_{corr} for the submerged-flow tests, and to compare those results to the previously developed ARS curve relating $E_{\text{corr}}/(y_2-y_j)$ and $(y_2-y_j)/y_j$. Only the data from Gates 1, 2, and 3 (hard rubber bar seal) and Gates 7, 8, and 9 (sharp edged) were used. The submerged-flow data for Gates 4, 5, and 6 (music note seals) were saved for verification testing.

The relative energy correction relation proposed by Clemmens et al. (2003) [left side of Eq. (7)] varies from 1.0 at $(y_2-y_j)/y_j=0$ to zero at $(y_2-y_j)/y_j>3.89$. At each extreme, E_{corr} itself approaches zero, since the relative energy correction computed from Eq. (7) must be multiplied by the depth increase, y_2-y_j, to obtain E_{corr}. The maximum effect of the energy correction actually occurs at intermediate values of the relative depth increase, in the region where the relative energy correction is changing rapidly. As mentioned earlier, Clemmens et al. (2003) speculated that the relative gate opening, w/H_1, might affect the energy correction relationship.

Although relative gate opening, w/H_1, is a convenient physical ratio, from a hydraulic standpoint a more appropriate dimensional ratio is the relative jet thickness at the vena contracta, y_j/H_1. Since different gate seals produce varying contraction behavior, two different gates set to the same relative gate opening might produce a different relative jet thickness, or alternately, two gates set to different openings might produce a flow with the same relative jet thickness if the contraction coefficients are also different. The important point is that the flow downstream from the gate should behave the same, regardless of how the final jet thickness is produced. Thus, we will use y_j/H_1 in the analysis that follows, and some implications of this will be discussed later.

Fig. 6 shows computed values of the relative energy correction, $E_{\text{corr}}/(y_2-y_j)$ versus the relative depth increase at the vena contracta, $(y_2-y_j)/y_j$, subdivided by ranges of y_j/H_1 values. Relationships between the energy correction and a jet Froude number and jet Reynolds number were also investigated, but were not consistent over the full range of the data. The E_{corr} and y_2 values are those obtained by iterative solution of the momentum and energy equations to obtain perfect prediction of the discharges observed in the Buyalski tests. The figure also shows the ARS fitted curve [Eq. (7)].

The general trend is for the transition zone of the energy correction curve to become steeper and shift to the left (toward lower values of the relative depth increase) as the y_j/H_1 ratio increases. Thus, when the gate exerts less control on the flow, transition occurs much more rapidly. There is some scatter in the data, including a small fraction of computed values of $E_{\text{corr}}/(y_2-y_j)$ that are greater than 1.0 or less than zero. These data are inconsistent with the physical meaning of the energy correction term and are attributed to experimental errors or anomalies. These data were excluded from later curve-fitting efforts.

The initial objective was to fit the ARS curve or an equation of a similar form to the Buyalski data for different y_j/H_1 ratios by changing the values of one or more of the four empirical factors in Eq. (7). This proved to be a difficult task. The objective in development of the ARS curve had been to obtain a function that passed through the point $E_{\text{corr}}/(y_2-y_j)=1$ at $(y_2-y_j)/y_j=0$, and approached a limit of $E_{\text{corr}}/(y_2-y_j)=0$ at larger values of $(y_2-y_j)/y_j$. Eq. (7) accomplished this with a relatively complex curve using an inverse tangent function and having an inflection point near $E_{\text{corr}}/(y_2-y_j)=0.5$. This functional form appeared to be somewhat compatible with the Buyalski data at large values of

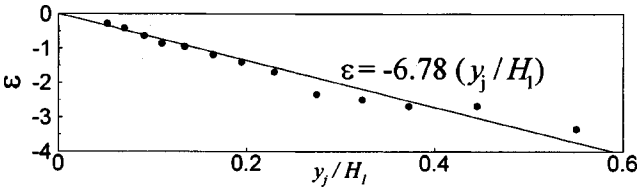

Fig. 7. Regression relation for parameter ε in Eq. (12)

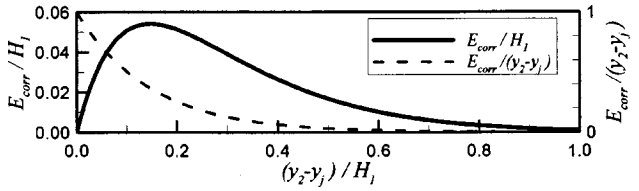

Fig. 9. Energy correction versus depth increase relative to upstream head

y_j/H_1, but for small values of y_j/H_1, it could not fit the data at intermediate values of $(y_2-y_j)/y_j$ and still pass through the point $(y_2-y_j)/y_j=0$ and $E_{corr}/(y_2-y_j)=1$. It is difficult to conclude independently from the Buyalski data that passage through the (0, 1) point is necessary because the Buyalski data set contains few points at very low values of $(y_2-y_j)/y_j$, but this requirement is compelling from a physical viewpoint.

After exploring several alternative equation forms, the most satisfactory model found for the energy correction relationship was a simple exponential power function of the form

$$\frac{E_{corr}}{y_2-y_j}=e^{\varepsilon[(y_2-y_j)/y_j]} \tag{13}$$

where ε=empirically determined coefficient; and e=base of natural logarithms. To fit these data to this relation, curve fitting was performed manually with the objective of minimizing the sum of the Pearson residuals, $\ln[(1+|\text{residual}|^2)^{0.5}]$. This approach minimizes the influence of outliers. This procedure produced good curve fits for most of the y_j/H_1 ranges, although a few were less than satisfying. Future research may better define the shape of the curve for low values of $(y_2-y_j)/y_j$.

A total of 13 bands of y_j/H_1 values were analyzed, and exponential functions were fitted for each range. Fig. 7 shows ε plotted versus the average y_j/H_1 values for each band. A linear regression yields the following final equation for $E_{corr}/(y_2-y_j)$, which replaces Eq. (7):

$$\frac{E_{corr}}{y_2-y_j}=e^{-6.78(y_j/H_1)[(y_2-y_j)/y_j]}=e^{-6.78[(y_2-y_j)/H_1]} \tag{14}$$

Note the cancellation of the y_j terms which takes place because we chose to analyze the energy correction as a function of the relative jet thickness, y_j/H_1, rather than the relative gate opening, w/H_1. If the analysis had been based on w/H_1, some simplification would have been possible by recognizing that $y_j=\delta w$, but the contraction coefficient, δ, would have remained embedded in the final equation, indicating that the energy correction factor was dependent on the contraction characteristics of the gate. Such an analysis was performed previously by Wahl et al. (2003). The form of Eq. (14) suggests that if we plot data for widely varying y_j/H_1 ranges as a function of $(y_2-y_j)/H_1$, rather than versus $(y_2-y_j)/y_j$ as was done in Fig. 6, we should obtain a single curve rather than a family of curves dependent on the relative jet thickness. Fig. 8 shows that this is generally the case, with just a few distinct bands of y_j/H_1 included on the plot for clarity. This also suggests that a single exponential function could be fit to all the data, rather than analyzing distinct bands of y_j/H_1 values. Doing so yields a slightly different coefficient (−6.75) in Eq. (14). By analyzing the data in bands, each range of y_j/H_1 values carries similar weight in the final result, even though the bands did not all contain the same number of data.

We can use Eq. (14) to examine the physical significance of the submerged-flow energy correction, E_{corr}, by computing values of $E_{corr}/(y_2-y_j)$ as $(y_2-y_j)/H_1$ varies from zero to 1, and then multiplying by the associated value of $(y_2-y_j)/H_1$ to obtain the value of E_{corr}/H_1 as a function of $(y_2-y_j)/H_1$ (Fig. 9). The maximum energy correction is about 5.5% of the upstream head and occurs when the depth increase at the vena contracta is about 15% of the upstream head.

One question that arises in evaluating the outcome of this analysis is the influence of the other empirical factors whose values may have affected the determination of E_{corr}. To evaluate this, some simple sensitivity analyses were performed. The values of the upstream energy loss factor, ξ, the contraction coefficient, δ, and the momentum equation weighting factor, p, were each changed individually by 5%, and E_{corr} values were then recomputed. The percentage change in the value of E_{corr} increases with the level of submergence, but at the point of maximum influence

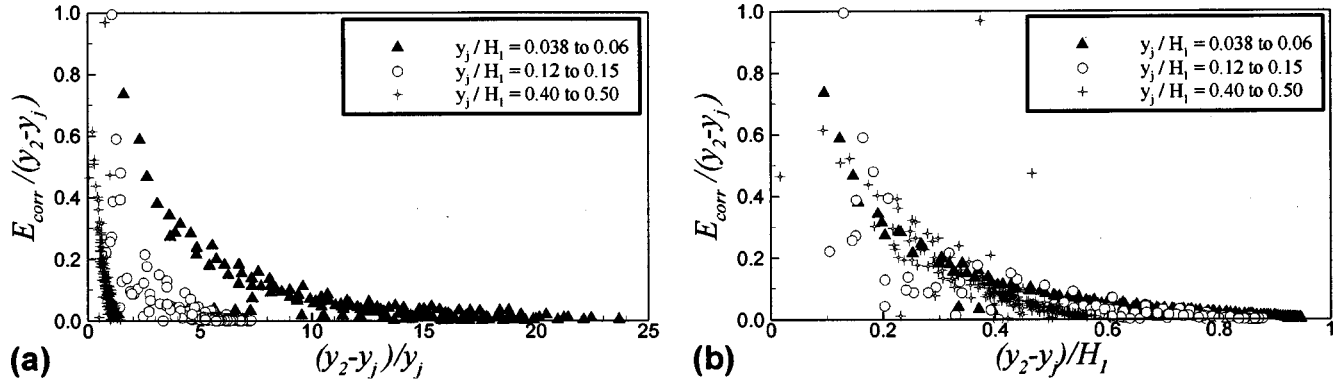

Fig. 8. Relative energy correction versus depth increase relative to: (a) jet thickness and (b) upstream energy head, for selected bands of y_j/H_1 values

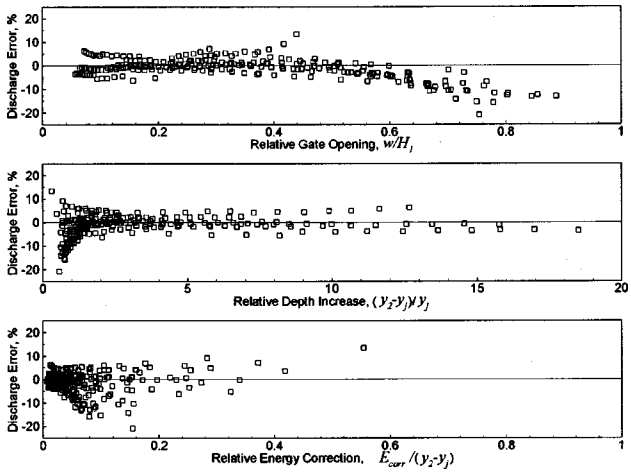

Fig. 10. Submerged-flow discharge prediction errors in verification test of the energy-momentum method with the refined energy correction model

of E_{corr} [approximately $(y_2-y_j)/H_1=0.15$, as explained in the previous paragraph], the changes in E_{corr} due to ξ, δ, and p were approximately 1.9, 44, and 1.6%, respectively. Clearly, it is important to know the contraction coefficient accurately, while uncertainties in the other two parameters have a much smaller, but still significant, influence on our determination of E_{corr}.

Verification Testing

To test the effect of refining the submerged-flow energy correction model, the *E-M* method was used to predict discharges for the Buyalski data from Gates 4, 5, and 6 (music note seals), computing the energy correction with Eq. (14) rather than Eq. (7). Both free-flow and submerged-flow cases were tested, although no changes had been made to the free-flow model. In free flow, 174 test runs were analyzed. Discharge was predicted within ±2% for 64% of the cases, and within ±5% for 99.4% of the cases. An error of +9% was obtained in one case; this test was reported to be submerged flow by Buyalski, but was modeled by the *E-M* method as free flow, so it is possible that there is an error in the data. The mean relative error was +0.40%, and the standard deviation of the relative errors was 1.97% (ignoring the one run just mentioned). These results are not quite as good as the initial test made against the free-flow data for the sharp-edged gates (Gates 7, 8, and 9), and the difference is most likely caused by additional uncertainty in the contraction coefficients of the music note seals. We should thus expect slightly larger errors in submerged flow as well.

The submerged-flow discharge prediction errors for 236 tests of gates with music note seals are shown in Fig. 10. To help illustrate the flow conditions that are the most error prone, the errors are plotted versus the relative gate opening, the relative depth increase, and the value of the relative energy correction, similar to the plots shown in Fig. 3 for the original *E-M* method applied to the sharp-edged gates. The error distribution is also compared in Table 2 to the results obtained with the original *E-M* model applied to the sharp-edged gates. There was significant improvement on all levels, and dramatic improvement in eliminating the very large errors that occurred when the flow is in the transition zone. The figure shows that there is no significant trend in the magnitude of errors as a function of the relative energy correction. This indicates significant improvement over the original *E-M* method for which Clemmens et al. (2003) reported that larger prediction errors occurred when the relative energy correction was in the range from 0.2 to 0.8 (the range in which the curve was relatively steep), as Fig. 3 confirmed.

Table 2. Comparison of Submerged-Flow Errors

	Percentage of observations	
Description	Original *E-M* model applied to sharp-edged Gates 7, 8, and 9 (%)	Modified *E-M* model applied to Gates 4, 5, and 6 (music note seals) (%)
±2% error	25	46
±5% error	66	78
±10% error	80	93
±20% error	86	99.6
+20 to +70% error	14	0.4
Percentage error statistics		
Mean error	+4.80	−1.35
Median error	−1.48	−0.75
Standard deviation	15.3	4.70

Note: *E-M* = energy-momentum.

To test the sensitivity of the *E-M* method to the influence of the weighting parameter, p, in the momentum equation, a sensitivity analysis was performed on the verification data set. For a change in p of 0.1, the resulting change in computed discharge (average of 236 runs from the verification data set discussed later in the paper) was about 0.4 to 0.5%. Thus, the influence on calibration accuracy of a reasonable variation of p was relatively slight.

It should be noted that the significant random scatter visible in Buyalski's free-flow data (Fig. 5) compared to that in the ARS data may carry over to the submerged-flow analysis as well. Thus, some of the scatter in Fig. 10 may be due to the quality of the Buyalski data set, and the *E-M* method may perform better with higher-quality data. The important point to remember is that a dramatic improvement was realized when the refined energy correction model was used.

Conclusions

With the refined energy correction model described here, the *E-M* method accurately predicts both free- and submerged-flow discharges through the model radial gates tested by Buyalski. Flow measurement uncertainties in free-flow conditions are about ±2% to ±5%. In submerged-flow conditions, the relative gate opening, w/H_1, plays an important role in determining the energy correction term needed for the energy equation. With the refined energy correction model, discharge in submerged-flow conditions is predicted with an uncertainty on the order of ±5% to ±10% in most cases. The largest errors still occur during conditions of slight submergence at large relative gate openings, but the magnitude of such errors has been reduced dramatically from as much as 70% to about 10%.

Several empirical parameters and relations are important to the performance of the *E-M* method. In free-flow conditions, the contraction coefficient and the energy loss and velocity distribution factor are the primary sources of uncertainty in the model, with the contraction coefficient being the dominant source of error. The Buyalski data set provided enough information to create useful

models for the contraction coefficients of the hard rubber bar seals and music note seals used on many prototype radial gates, but further improvement is certainly possible, and variability in the characteristics of these types of seals on prototype gates is likely to be significant. The Buyalski free-flow data were not able to shed much additional light on the energy loss and velocity distribution factor, although many of the tests were carried out at larger Reynolds numbers than those attained in previous work by ARS. The equation proposed by Clemmens et al. (2003) appears to be the best available relation. This is a question of importance for field applications, since most prototype gates will have much larger Reynolds numbers than those used to develop the model for the energy loss and velocity distribution factor, but fortunately $1+\xi$ approaches a limiting value of 1.0 at large Reynolds numbers.

In submerged flow, the additional factor that is of great importance is the energy correction term. The model proposed by Clemmens et al. (2003) was refined, yielding a relation that incorporates the significant effects of the relative gate opening. The form of the energy correction relation proposed here differs significantly from that proposed by Clemmens et al. (2003), and additional experimental data are needed to verify the behavior of the energy correction at the beginning of the transition into submerged flow [low values of $(y_2-y_j)/y_j$].

The analysis performed here did not produce any change in the empirical weighting factor, p, used to estimate forces on the downstream channel walls needed for the momentum equation. Buyalski's test channel was relatively narrow compared to that used in the ARS tests, but was otherwise similar, so it is still possible that other geometries will require significant adjustment of the value of p. Features such as bed drops downstream from the gate or flared transitional walls may prove to be important.

Acknowledgments

The writer thanks Dr. Albert Clemmens and the anonymous reviewers of this manuscript for their insightful suggestions on the analysis of these data and the preparation of this paper. The work performed here would never have been possible without the extensive set of laboratory data collected by Mr. Clark Buyalski. His perseverance and thoroughness in the collection and publication of these data are exemplary. The work reported here was funded by Reclamation's Science and Technology Program as part of the *Flow Measurement with Canal Gates* project.

Notation

The following symbols are used in this paper:

a = gate trunnion pin height above base of gate chamber;
b_1 = upstream channel width;
b_c = gate width;
E_{corr} = submerged-flow energy correction;
e = base of natural logarithms, 2.718282;
F_3 = hydrostatic force on downstream control volume boundary;
F_w = force exerted by upstream channel boundaries surrounding gate;
g = acceleration of gravity;
H = total energy head;
p = weighting factor used to compute y_w;
Q = discharge;
R = Reynolds number;
R_h = hydraulic radius immediately upstream from gate;
r = gate radius;
V = characteristic velocity at entrance to gate opening;
v = flow velocity;
v_e = effective velocity in vena contracta jet in submerged flow;
w = vertical gate opening;
y = flow depth;
y_j = jet thickness at the vena contracta;
y_w = effective water depth used to estimate F_w;
α = velocity distribution coefficient;
ΔH = energy loss;
δ = contraction coefficient;
ε = empirically determined exponent;
θ = gate lip angle from horizontal;
ν = kinematic viscosity;
ξ = energy loss coefficient; and
ρ = fluid density.

Subscripts

1 = sections upstream from the gate;
2 = sections at the vena contracta;
3 = sections downstream from the gate; and
$_j$ = conditions in the vena contracta jet.

References

Buyalski, C. P. (1983). "Discharge algorithms for canal radial gates." *Research Report REC-ERC-83-9*, Bureau of Reclamation, Denver, Available on the web at ⟨http://www.usbr.gov/pmts/hydraulics_lab/pubs/REC/REC-ERC-83-09.pdf⟩.

Clemmens, A. J., Strelkoff, T. S., and Replogle, J. A. (2003). "Calibration of submerged radial gates." *J. Hydraul. Eng.*, 129(9), 680–687.

Tel, J. (2000). "Discharge relations for radial gates." MSc. thesis, Delft Technical Univ., Delft, The Netherlands.

Toch, A. (1955). "Discharge characteristics of tainter gates." *Trans. Am. Soc. Civ. Eng.*, 120, 290–300.

Wahl, T., Clemmens, A. J., and Replogle, J. A. (2003). "The energy correction for calibration of submerged radial gates." *Proc. 2nd Int. Conf. Irrigation and Drainage*, USCID, Phoenix.